Paper No.
19

CORROSION96
The NACE International Annual Conference and Exposition

PREDICTIVE MODEL FOR SWEET CORROSION IN HORIZONTAL MULTIPHASE SLUG FLOW

W. P. JEPSON, S. BHONGALE, AND M. GOPAL
NSF, I/UCRC CORROSION IN MULTIPHASE SYSTEMS CENTER
DEPARTMENT OF CHEMICAL ENGINEERING
OHIO UNIVERSITY
ATHENS, OHIO
USA

ABSTRACT

Experiments have been performed in a 10 cm ID horizontal pipeline to observe the effect of temperature, carbon dioxide partial pressure, flow, and oil/water composition, on corrosion in horizontal multiphase slug flow, using a low viscosity (2 cp) oil. Corrosion rates have been measured for water cuts ranging form 20 to 100%, carbon dioxide partial pressures of 0.27, 0.45 and 0.79 MPa, temperatures of 40, 60, 70, 80 and 90 C and Froude numbers of 6, 9 and 12. The corrosion rates are found to increase with an increase in temperature, Froude number and carbon dioxide partial pressure. The corrosion rates are found to decrease with increase in oil composition. The average void fraction as well as the pressure drop across the slug is found to increase with an increase in Froude number and carbon dioxide partial pressure. A model to predict corrosion rates for low viscosity oils has been established which relates the corrosion rate to the pressure gradient, temperature, carbon dioxide partial pressure and water cut.

Keywords: Horizontal Multiphase Flow, Corrosion, High Pressure, Carbon Steel, Prediction, Model.

INTRODUCTION

When the oil fields are located in remote areas such as Alaska or subsea, it is not practical to separate the oil/water/gas at the well site. Hence, it is a common practice to transport the oil/water/gas mixture from several wells to a central gathering station through large diameter pipelines, where separation takes place.

As the well ages, enhanced methods of oil recovery involving the injection of carbon dioxide and water are used. This helps to maintain the pressure within the reservoir. However, some of the carbon dioxide and brine flows with the oil and gas. This multiphase flow of oil-water-gas mixture creates a number of corrosion problems in the pipelines. Many oil wells operate at high water cuts, as high as 80%. Also, in the presence of water, the added carbon dioxide forms weak carbonic acid. This acid being corrosive in nature, causes higher corrosion rates in carbon steel pipelines. The oil and gas mixture may also contain waxes, hydrates, hydrogen sulphide and sand.

Several predictive models for the corrosion rate have been developed. De Waard and Milliams (1975)[1] performed corrosion studies in stirred beakers and determined corrosion rates by means of weight loss coupons and polarization resistance measurements. They studied the effect of carbon dioxide partial pressure and temperature on corrosion. They found that the corrosion rate initially increases with increase in temperature from 30 to 60 C, reaches a maximum between 60 to 70 C and thereafter decreases until 90 C. Similar results were also obtained by Vuppu and Jepson (1994)[2] who performed experiments in flow loops under full pipe flow conditions. Also, the corrosion rates increased with increase in carbon dioxide partial pressure. De Waard and Milliams proposed a predictive model for corrosion rates which incorporated the effects of pressure and temperature. However, this model did not take into account the effects of flow velocity, presence of corrosion products on the metal surface and oil composition.

Later, an improved model, which provided correction factors for the non-ideality of carbon dioxide at high pressures, formation of iron carbonate scales at high temperatures and changes in pH and Fe^{2+} ion levels, was presented by de Waard, Lotz and Milliams (1991)[3]. They later (1993)[4] presented a revised correlation between corrosion rate and flow velocity, temperature and carbon dioxide partial pressure. Based on the experiments performed in a high pressure test loop, de Waard, Lotz and Dugstad (1995)[5] proposed a semi-empirical model for corrosion rates. This model combined the contribution of flow-independent kinetics of the corrosion reaction with one from flow dependent mass transfer of dissolved carbon dioxide by means of a resistance model. This model still did not take into account the effect of oil composition.

Efird, Wright, Boros and Hailey (1993)[6] performed experiments with three different systems, 2.54 cm and 9 cm pipe diameter loops, jet impingement, and rotating cylinder electrode method. They established a correlation between corrosion rate and wall shear stress. This correlation is given by the following equation:

$$R_{COR} = a\ \tau_w^{\ b} \qquad (1)$$

where, R_{COR} = corrosion rate in mm/year
τ_w = wall shear stress in N/m^2
a & b = constants

This equation is valid only for brine and different values of a and b are needed if it is to be applied to other systems. The value of the coefficient "a" varied with the temperature, carbon dioxide partial pressure and the type of flow. These tests also provided a comparison between pipe flow, rotating cylinders and the jet impingement technique. It was found that the pipe flow correlated better with the jet impingement technique, while the results from rotating cylinders grossly underestimated the corrosion rates.

Kanwar and Jepson (1994)[7] performed corrosion studies in a 10 cm diameter flow loop under full

pipe flow conditions, at carbon dioxide partial pressures up to 0.79 MPa, temperature of 40 C with two oils of viscosities 2 and 18 cp and ASTM water. Based on the concept introduced by Efird et al.(1993), they proposed the following predictive model for corrosion rate:

$$R_{COR} = k\, P^{c}\, \tau_{w}^{\,b} \qquad (2)$$

where, R_{COR} = corrosion rate in mm/year
P = carbon dioxide partial pressure in MPa
τ_w = wall shear stress in N/m^2
b & c = constant exponents with values of 0.1 and 0.83 respectively
k = constant $(mm/year)(MPa)^{-0.83}(N/m^2)^{-0.1}$

This relation is valid for full pipe flow of low viscosity oils with concentrations up to 60% oil and a temperature of 40 C. Later, Kanwar (1994)[8] carried out similar experiments at temperatures of 30, 33, 50 and 60 C to determine the effect of temperature on the corrosion rate. He found that the coefficient "k" in above equation 2, could be represented as a function of temperature in the following manner:

$$k(T) = k_1\, T\, e^{\left(-\frac{5041}{T}\right)} \qquad (3)$$

where, k_1 = constant with value 416649 $(mm/year)(MPa)^{-0.83}(N/m^2)^{-0.1}(K)^{-1}$
T = temperature in Kelvin

However, this equation cannot be applied at temperatures higher than 60 C, since it does not account for the formation of protective iron carbonate scales at these higher temperatures.

The present work focuses on the effect of flow, temperature, carbon dioxide partial pressure and oil composition on the corrosion rate in horizontal multiphase slug flow.

EXPERIMENTAL SETUP AND PROCEDURE

The experimental setup is shown in Figure 1. The system is made of 316 stainless steel and is designed to withstand a maximum pressure of 100 bars. A predetermined oil-water mixture is stored in a 1.2 m^3 tank which serves as a storage tank as well as a separation unit for the multiphase gas-oil-water mixture. The system temperature is controlled by two 1.5 kW heaters, connected to a thermostat. The liquid is pumped by a 5.2 kW stainless steel, centrifugal pump into a 7.72 cm ID pipeline. An orifice plate is used to measure the flow rate. The pressure drop across the orifice plate is measured with a manometer. The liquid flow rate is controlled by adjusting the gate valve C on the bypass line, and valve D. The bypass also serves to keep the two liquid phases well mixed in the storage tank.

The liquid then passes into a 10.16 cm ID pipeline where carbon dioxide enters at the point H. The gas/liquid mixture flows through the test section and back into the holding tank where the gas and liquid are separated. A back pressure regulator K, maintains the pressure in the system. The gas flow rate is controlled by a needle valve.

The test section is shown in Figure 2. The openings E and C at the top and the bottom of the pipe are used to flush mount the ER probes with the pipe wall for the corrosion rate measurement, and the coupon holder probes for weight loss measurements and for performing morphological studies using Scanning Electron Microscopy (SEM). The positions P are pressure tappings, which are connected to a pressure

transducer and are used to measure the pressure drop between various locations in the test section. S is a port for the insertion of a shear stress probe but is not used in this work. ST is the sampling probe used to take out samples of the flowing fluid to determine oxygen, iron and carbon dioxide concentrations in the system.

The fluids used were a refined oil with a viscosity of 2 cp at 40 C and density of 800 kg/m^3 and ASTM standard sea water. Carbon dioxide is used as the gas phase.

The experiments were performed at carbon dioxide partial pressures of 0.27, 0.45 and 0.79 MPa, temperatures of 40, 60, 70, 80 and 90 C and a Froude number of 6, 9 and 12 (corresponding to slug velocities of 3, 4.5 and 6 m/s respectively). Water cuts of 100, 80, 60, 40 and 20% were used.

The Froude number is defined as follows:

$$Fr = \frac{v_t - v_{LF}}{\sqrt{g h_{EFF}}} \qquad (4)$$

where,

Fr	=	Froude number in the liquid film ahead of the slug
v_t	=	translational velocity of the slug, m/s
v_{LF}	=	velocity of the liquid film ahead of the slug, m/s
g	=	acceleration due to gravity, m/s^2
h_{EFF}	=	effective height of the liquid film ahead of the slug, m

RESULTS

Figure 3 shows the effect of temperature on corrosion rate for brine at Froude numbers of 9 and 12, and carbon dioxide partial pressures of 0.27, 0.45 and 0.79MPa. It is seen that at each of the carbon dioxide partial pressures and Froude numbers, the corrosion rate increases with an increase in temperature. No maximum in the corrosion rate is seen at any of the temperatures studied. For example, at a carbon dioxide partial pressure of 0.79MPa and Froude number of 9, the corrosion rate increases from 12.1 to 34.1 mm/year with increase in temperature from 40 to 60 C, then increases at a slower rate from 34.1 to 38.2 mm/year with increase in temperature from 60 to 70 C and finally increases at a much higher rate from 38.2 to 63.5 mm/year with further increase in temperature from 70 to 90 C. This is not seen in the results obtained by de Waard and Milliams (1975), wherein a maximum in the corrosion rate was observed at a temperature between 60 to 70 C. However, for slug flow, the higher rate of increase in corrosion rate with temperature above 70 C, could be due to possible stripping away of the protective layer of corrosion products on the metal surface, due to high levels of shear and turbulence encountered in slug flow. This is also confirmed from the morphological studies, using SEM of the coupon surfaces, where the average thickness of the corrosion product layer on the slug flow coupons is found to be much smaller than the average thickness found on full pipe flow coupons.

Figure 4 shows similar results obtained for lower water cuts of 80%. It is seen that the corrosion rate increases almost linearly with increase in temperature. Similar results are seen for water cuts of 60 and 40%.

The variation of corrosion rate with oil composition at a Froude number of 12, temperatures of 40, 60 and 80 C and carbon dioxide partial pressure of 0.79MPa is shown in Figure 5. At a temperature of 80 C, the corrosion rate decreases from 58.5 to 48.5 mm/year with increase in oil composition from 0 to 40%, then decreases at a higher rate from 48.5 to 33.5 mm/year with increase in oil composition from 40 to 60%

and finally reduces to negligible value for oil composition of 80%. Figure 6 shows the variation of the oil fraction across the pipe diameter for a water cut of 80% at carbon dioxide partial pressure of 0.79MPa. It is seen that the oil fraction is almost uniform across the pipe diameter indicating that the liquid phase is well mixed under slug flow conditions. The oil is now the continuous phase at this percentage of oil in the liquid. Hence, with increase in oil composition, less water contacts the pipe surface leading to decrease in corrosion rate. Also, from Figure 7 which shows the void fraction at the bottom of the pipe it can be seen that the void fraction here at the bottom of the pipe deceases with increase in oil composition. This results in a decrease in the intensity of turbulence, resulting in the decrease in the corrosion rates.

Figure 8 shows the corrosion rate versus Froude number at temperatures of 40, 60 and 80 C, carbon dioxide partial pressures of 0.27 and 0.79 MPa and water cut of 80%. It is seen that at each temperature and carbon dioxide partial pressure, the corrosion rate increases with an increase in Froude number. For example, at a water cut of 80%, the corrosion rate increases from 28.1 to 31.9 to 34.4 mm/year with increase in Froude number from 6 to 9 to 12. The variation of the average void fraction across the pipe diameter with Froude number is shown in Figure 9 for water cut of 80%. The average void fraction increases with increase in Froude number, indicating that more and more gas is entrained in the slug. Also, from Figure 10 it is seen that the pressure drop across the slug in this case increases with increase in Froude number. Thus with increase in Froude number there is an increase in the intensity of shear and turbulence at the bottom of the pipe.

Since, the pressure drop across the slug is a measure of the shear and turbulence at the bottom of the pipe, the corrosion rates at each temperature were plotted against the experimentally obtained pressure gradients. Figure 11 and 12 show these plots for brine at carbon dioxide partial pressure of 0.27 and 0.79MPa respectively. It is found that, under almost all conditions the value of the exponent remains constant and its value is found to be 0.30±0.05. Similar results were obtained at lower water cuts of 80, 60 and 40%. So the following relation between the corrosion rate and the pressure gradient is proposed:

$$CR = a\left(\frac{\Delta P}{L}\right)^{0.3} \qquad \textbf{(5)}$$

However, it is found that the value of the coefficient 'a' varies with water cut, carbon dioxide partial pressure and temperature. Hence, the value of the coefficient 'a' was plotted against overall water cut at each of the temperatures of 40, 60 and 80 C. Figure 13 and 14 show these plots for carbon dioxide partial pressures of 0.27 and 0.79MPa respectively. In each case a power curve fit was made. It can be seen that the value of the exponent did not change much with temperature and carbon dioxide partial pressure. Its value is found to be 0.60±0.08. Thus the following relationship between the corrosion rate and overall water cut is obtained.

$$CR = c\left(\frac{\Delta P}{L}\right)^{0.3} v^{0.6} \qquad \textbf{(6)}$$

The value of the coefficient 'c' is seen to increase with increase in carbon dioxide partial pressure. These results suggested plots of the coefficient 'c', for different water cuts, against carbon dioxide partial pressure at each of the temperatures. These plots are shown in Figure 15. Once again a power curve fit was

made and it was found that the value of the exponent in each case was approximately 0.8. The coefficient, however, increased with increase in temperature. Hence, the equation for corrosion rate as a function of carbon dioxide partial pressure, water cut and pressure gradient becomes,

$$CR = k(T) \left(\frac{\Delta P}{L} \right)^{0.3} \nu^{0.6} P_{CO2}^{0.8} \quad (7)$$

The effect of temperature is now considered. As has been discussed previously, the corrosion rate increased with temperature over the entire range of temperatures studied. The transition theory is used to incorporate the effect of temperature into the model. From transition theory, it is known that the corrosion rate varies with temperature in the following manner,

$$CR = k_1 \, T \exp(- \frac{E}{RT}) \quad (8)$$

The value of the coefficient k(T) from equation is plotted against temperature. A regressional analysis of the values of k(T), was carried out to evaluate the activation energy constant 'E'. This is shown in Figure 16. The resulting equation defines the value of the constant k_1 and the activation energy. These values are,

$$E/R = 2671 \text{ K}$$
$$k_1 = 31.15$$

Thus the final expression for the corrosion rate as a function of pressure gradient, water cut, carbon dioxide partial pressure and temperature is given below.

$$CR = 31.15 \left(\frac{\Delta P}{L} \right)^{0.3} \nu^{0.6} P_{CO2}^{0.8} \, T \, e^{(- \frac{2671}{T})} \quad (9)$$

This is a predictive equation for corrosion rates for low viscosity oils under slug flow conditions. Figure 17 shows the graph of predicted corrosion rates versus the actual corrosion rates. The results are quite satisfactory and the predictions are good representations of the experimental data. Experiments are now being carried out to study corrosion rates for high viscosity oils under similar conditions.

Figure 18 compares the plot of corrosion rate obtained experimentally in this study and those predicted by the model of de Waard et al. (1995), versus temperature at a carbon dioxide partial pressure of 0.27 MPa. It can be seen that the de Waard et al. predictions are much lower than the experimental values obtained in this study under similar operating conditions. Figure 19 shows a similar comparison at a Froude number of 12 (liquid velocity of 6 m/s) and a temperature of 80 C. Here it can be seen that at higher carbon dioxide partial pressures, the de Waard et al. predictions are much lower than those obtained experimentally at the same operating conditions.

CONCLUSIONS

For the low viscosity oil tested, the corrosion rate increased with an increase in temperature over the

entire range studied, at every Froude number, carbon dioxide partial pressure and water cut. No maximum in the corrosion rate is observed at any of the temperatures studied. The high levels of shear and turbulence at the bottom of the pipe, encountered in slug flow, strip away the protective film of corrosion products formed on the pipe wall resulting in high rates of corrosion.

At each temperature, carbon dioxide partial pressure and water cut, the corrosion rate increased with an increase in Froude number. Also, with increase in Froude number, there was a increase in the void fraction at the bottom of the pipe as well as the average void fraction across the pipe diameter. This was manifested in an increase in the pressure drop across the slug indicating that the intensity of shear and turbulence increased with increase in Froude number.

The corrosion rate decreased with an increase in oil composition from 0 to 60%. The corrosion rate reduced to negligible values for an oil composition of 80%. This was due to the transition from a water continuous phase to an oil continuous phase. No maximum in the corrosion rate was seen at any of the oil compositions studied.

The oil fraction across the pipe diameter is more or less uniform across the pipe diameter indicating that the liquid phase is well mixed under slug flow conditions.

For slug flow, the pressure gradient is a measure of the shear and turbulence at the bottom of the pipe. A model to predict corrosion rates has been established which shows that the corrosion rates are dependent on the temperature, carbon dioxide partial pressure, pressure gradient across the slug and water cut. This model can predict corrosion rates up to water cuts of 60% for a low viscosity oil, carbon dioxide partial pressures up to 0.79 MPa and temperatures up to 90 C.

REFERENCES

1. De Waard C., and Milliams, D.E. "Carbonic Acid Corrosion of Steel", Corrosion, 31, 5(1975): p. 177.

2. Vuppu, A.K. and Jepson, W.P., "Study of Sweet Corrosion in Horizontal Multiphase, Carbon Steel Pipelines," Offshore Technology Conference, 7494/265-7494/276, (Houston, TX:SPE, 1993).

3. De Waard, C., Lotz, U., and Milliams, D.E., " Predictive Model for CO_2 Corrosion Engineering in Wet Natural Gas Pipelines," Corrosion, 47, 12(1991): p. 976.

4. De Waard, C., Lotz, U., and Milliams, D.E., "Prediction of CO_2 Corrosion of Carbon Steel," Corrosion/93, paper no. 69, (Houston, TX: NACE International, 1993)..

5. De Waard, C., Lotz, U., and Dugstad, D., "Influence of Liquid Flow Velocity on CO_2 Corrosion: A Semi-Empirical Model," Corrosion/95, paper no. 128, (Houston, TX: NACE International, 1995).

6. Efird, K.D., Wright, E.J., Boros, J.A., and Hailey, T.G. "Wall Shear Stress and Flow Accelerated Corrosion of Carbon Steel in Sweet Production," 12th International Corrosion Congress, Technical Paper TS 14 194, (Houston, TX: NACE International, 1993).

7. Kanwar, S., and Jepson, W. P., "A Model to Predict Sweet Corrosion of Multiphase Flow in Horizontal

Pipelines", Corrosion/94, paper no. 24, (Houston, TX: NACE International, 1994).

8. Kanwar, S. (1994). Study and Modeling of Sweet Corrosion of Multiphase Mixtures in a Horizontal Pipeline. Master's Thesis, Ohio University, Russ College of Engineering and Technology.

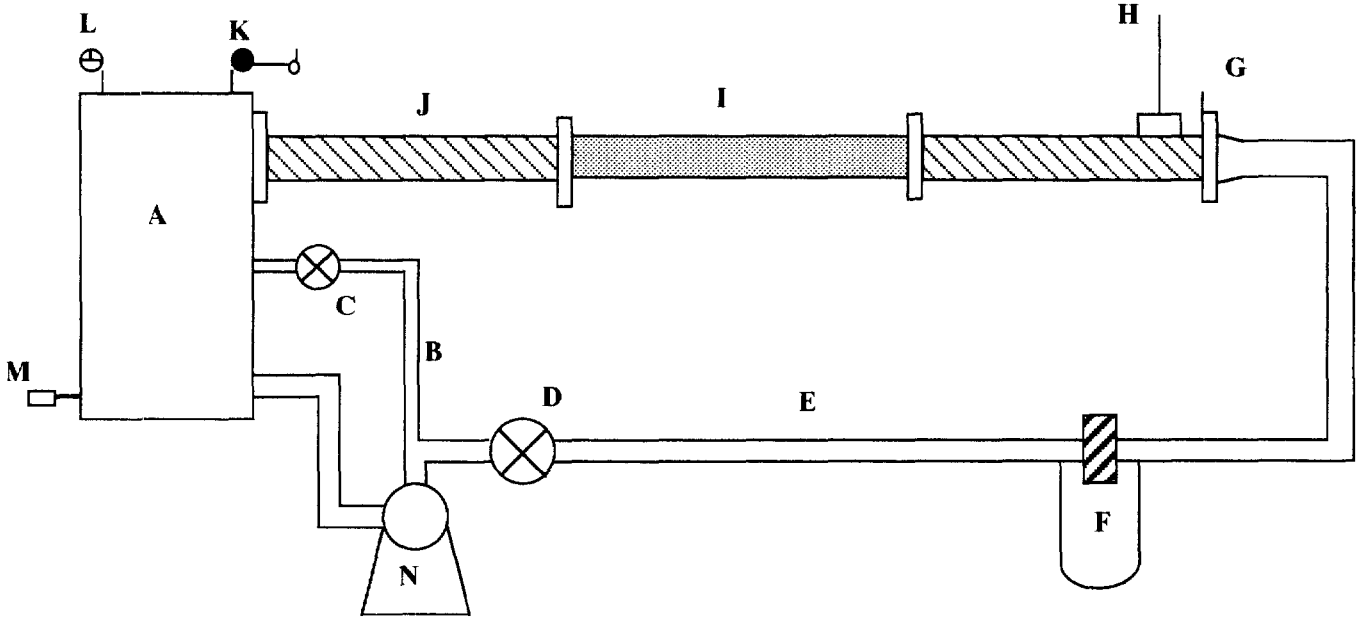

A. Liquid Tank
B. Liquid Recycle
C. Valve on Liquid Recycle
D. Valve on Liquid Feed
E. Liquid Feed- 7.6 cm Stainless Steel Pipe
F. Orifice plate, to pressure transducer
G. Flow Height Control Gate
H. Carbon dioxide Feed Line
I. Test Section- 10.16 cm Stainless Steel pipe
J. 10.16 cm Stainless Steel Section
K. Pressure Gauges & Back Pressure Regulator
L. Safety valve
M. Heater
N. Pump

Figure 1. Layout of The Experimental System

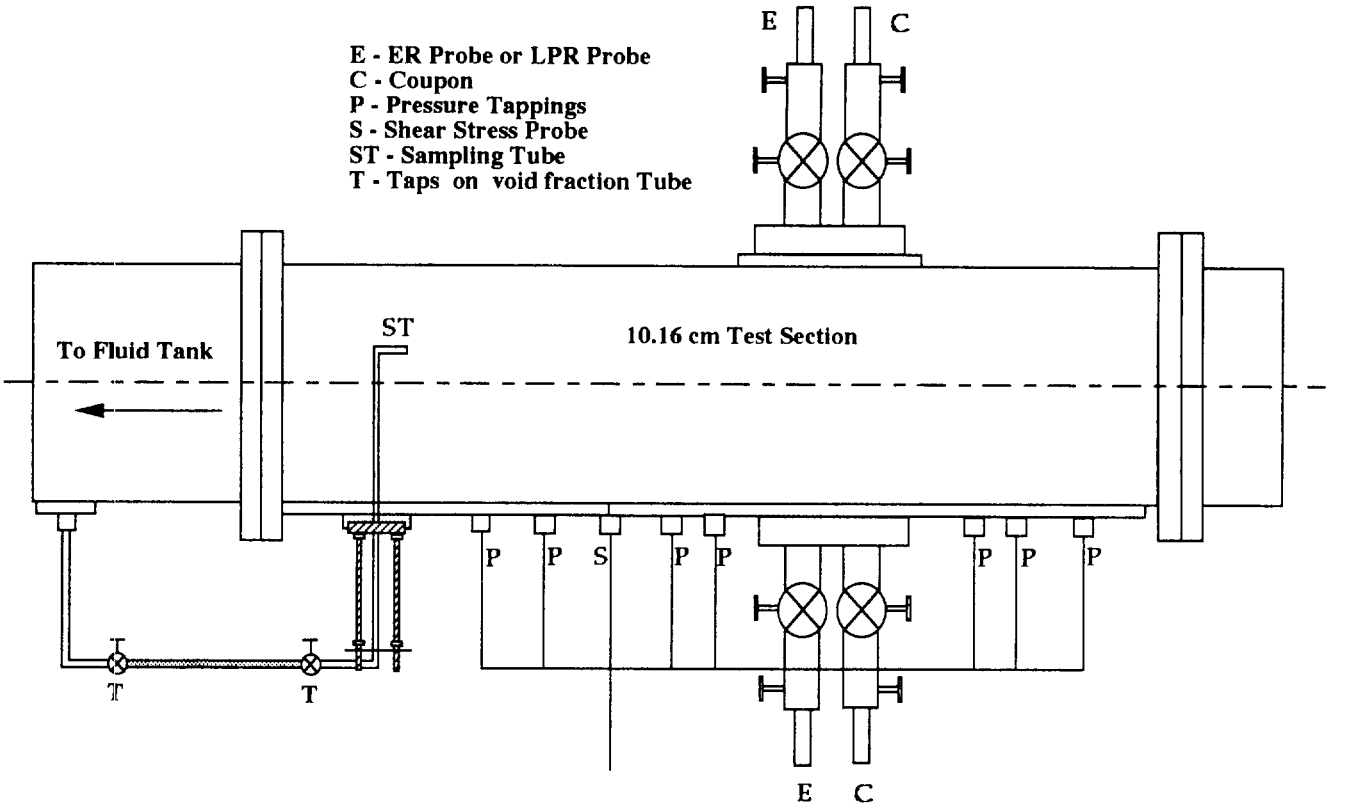

Figure 2. Test section

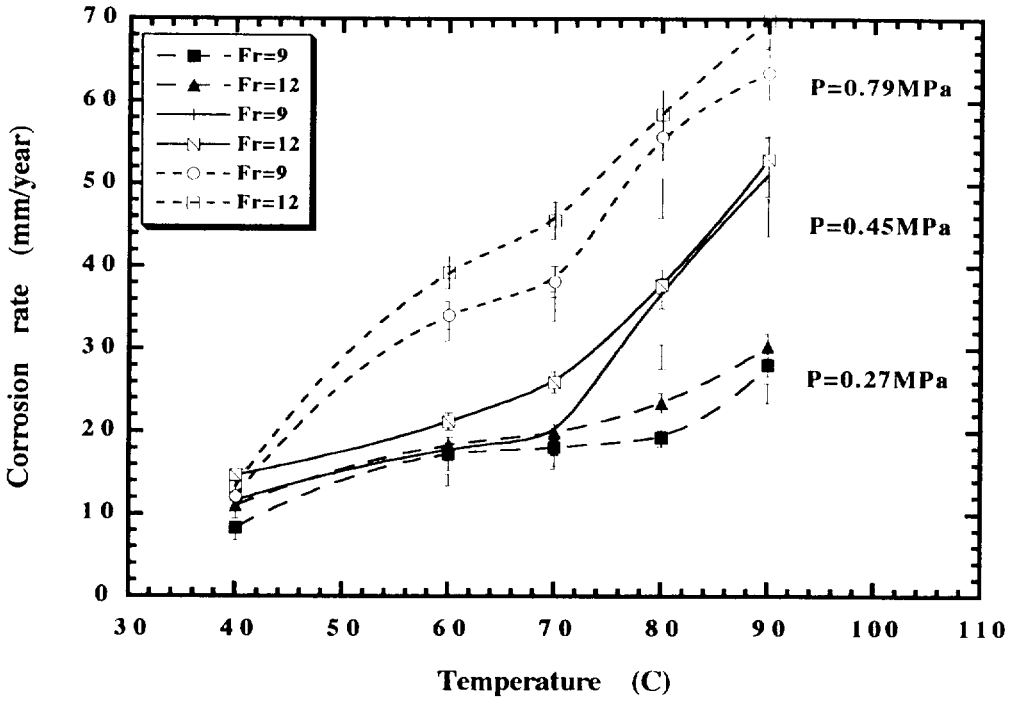

Figure 3. Corrosion rate vs Temperature for brine

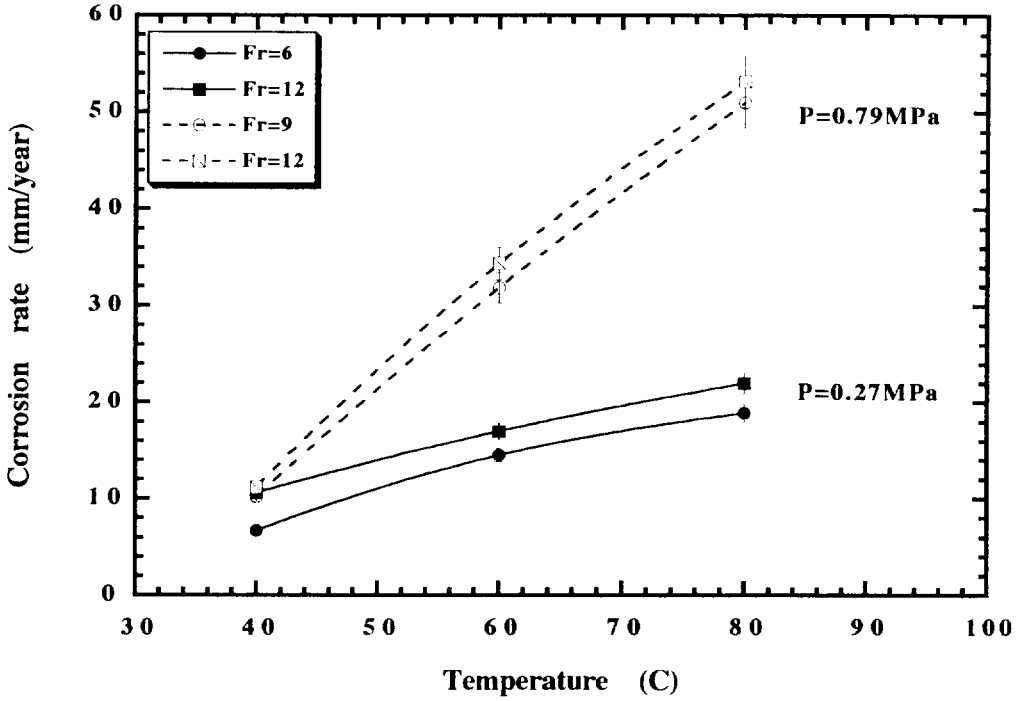

Figure 4. Corrosion rate vs Temperature for 80% water cut

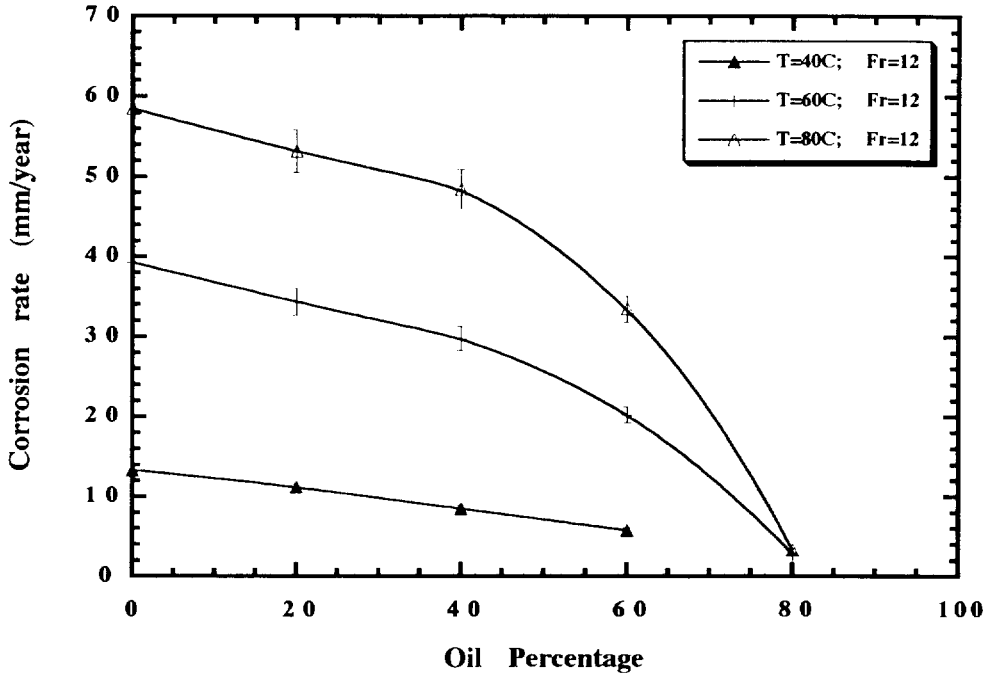

Figure 5. Corrosion rate vs Oil composition at CO_2 partial pressure of 0.79MPa and Froude number of 12.

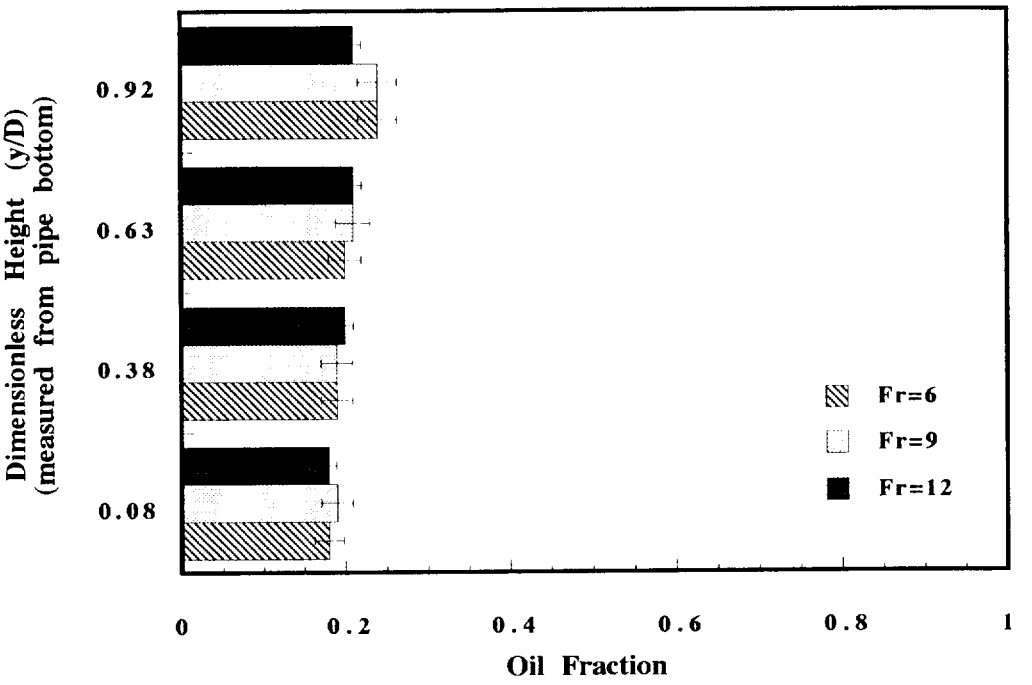

Figure 6. Oil fraction across the pipe diameter for 80% water cut at CO_2 partial pressure of 0.79MPa

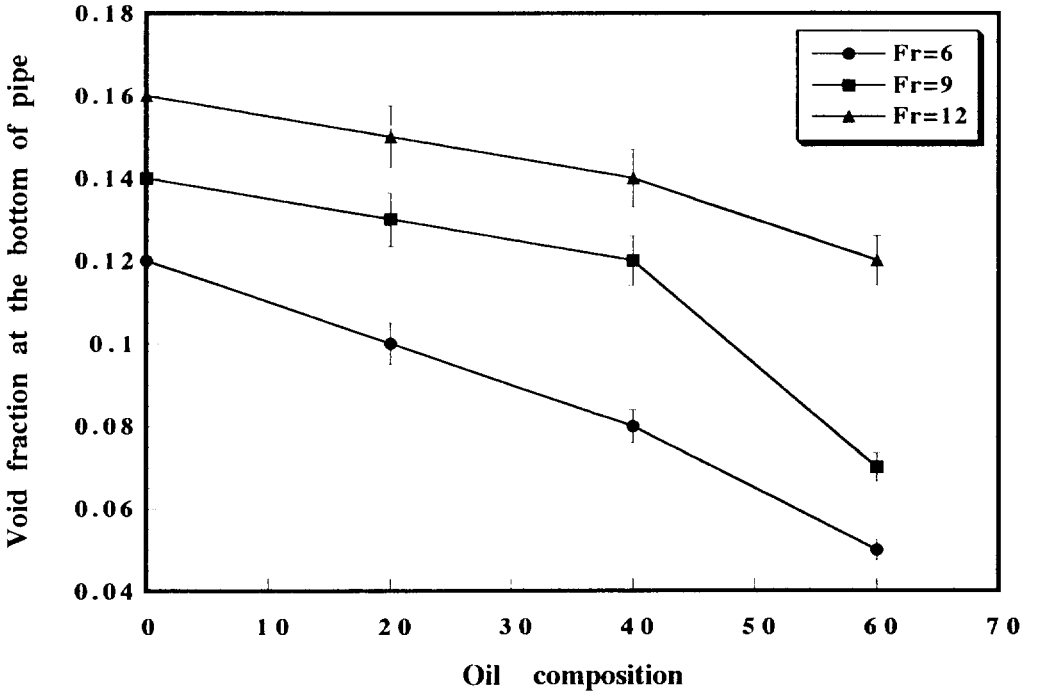

Figure 7. Void fraction at the bottom of the pipe vs Oil composition at CO_2 partial pressure of 0.79MPa

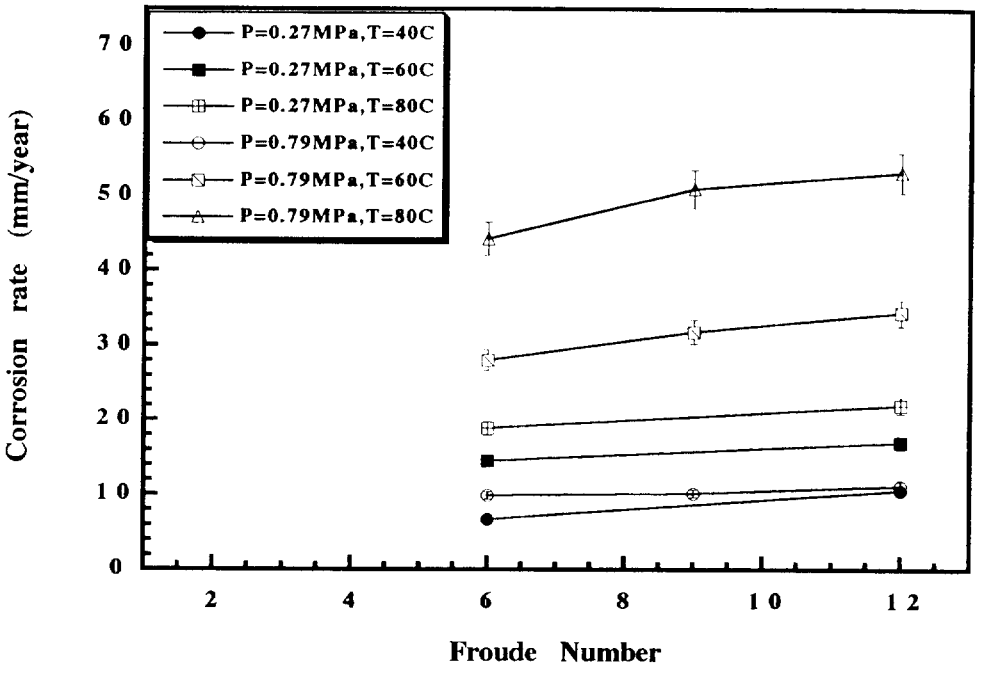

Figure 8. Corrosion rate vs Froude number for 80% water cut

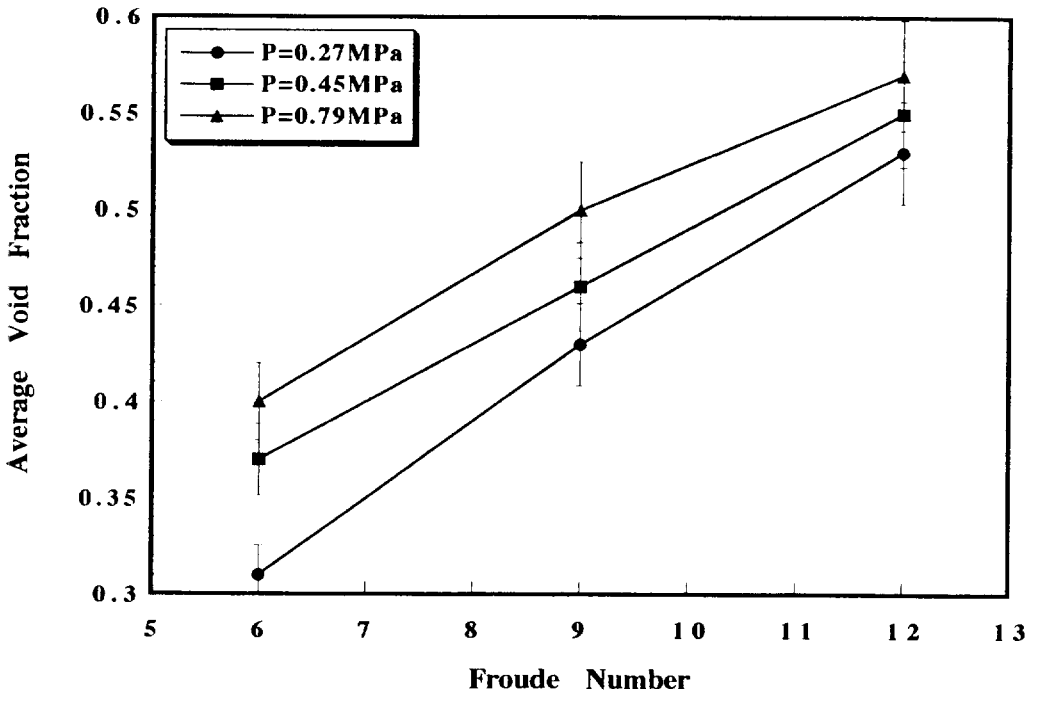

Figure 9. Average Void fraction across the pipe diameter vs Froude number for 80% water cut

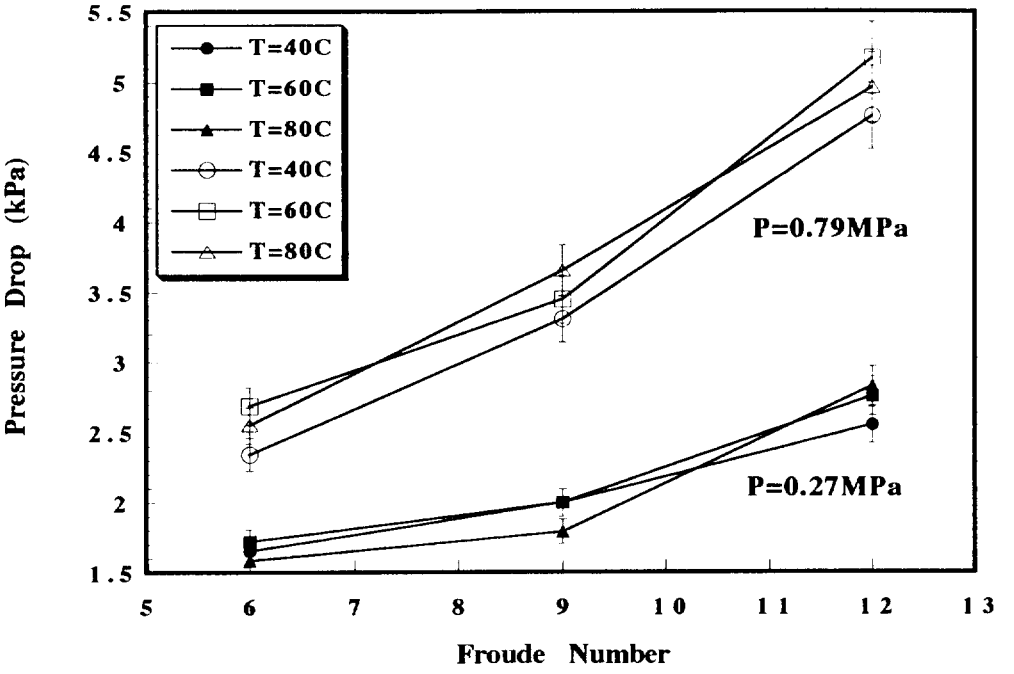

Figure 10. Pressure drop across the slug vs Froude number for 80% water cut

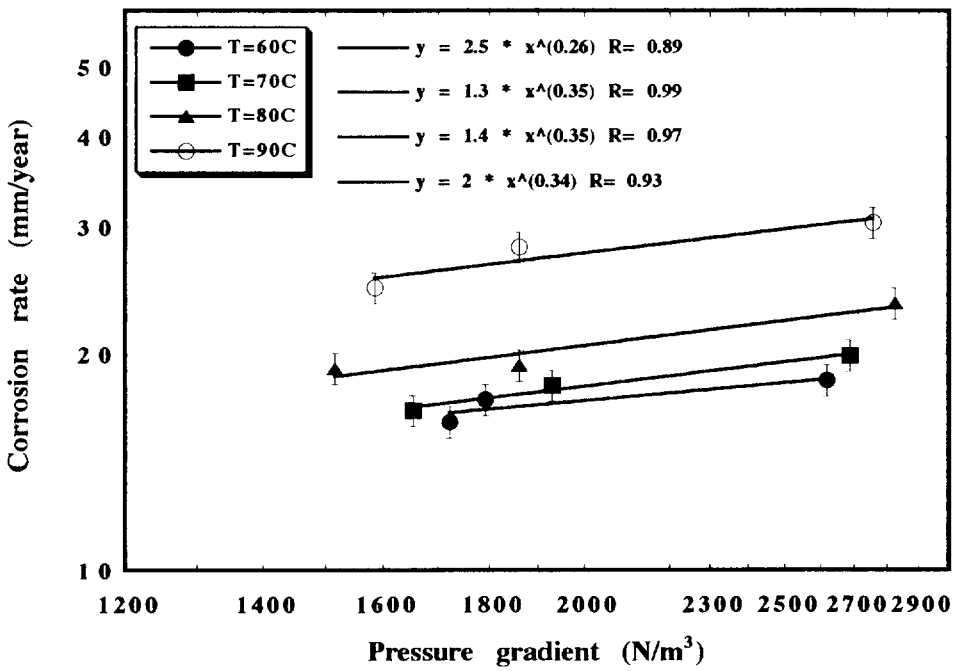

Figure 11. Corrosion rate vs Pressure gradient for brine at carbon dioxide partial pressure of 0.27MPa

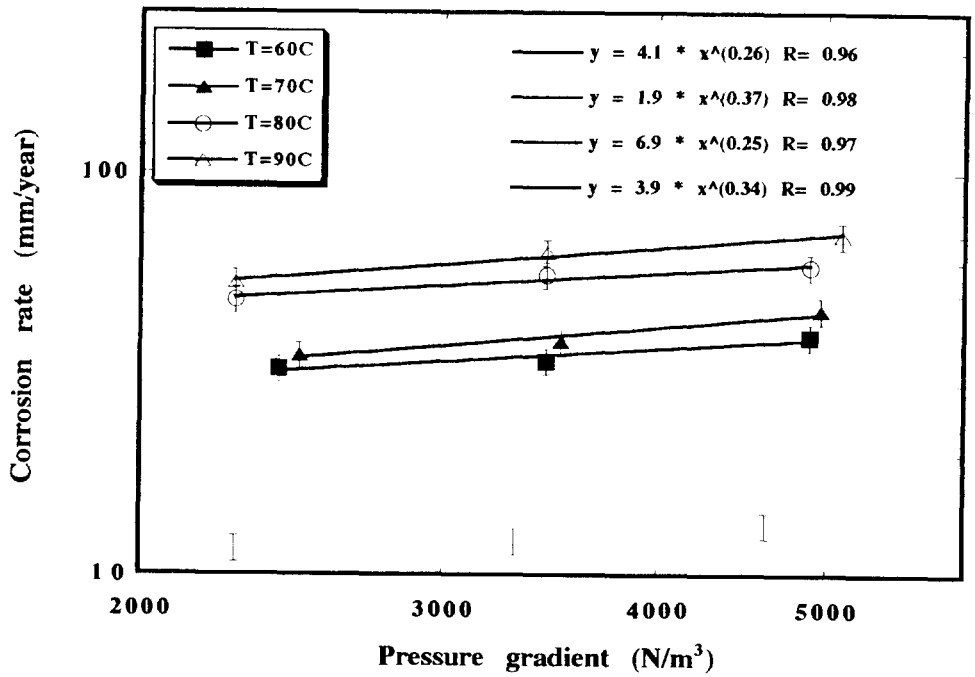

Figure 12. Corrosion rate vs Pressure gradient for brine at carbon dioxide partial pressure of 0.79MPa

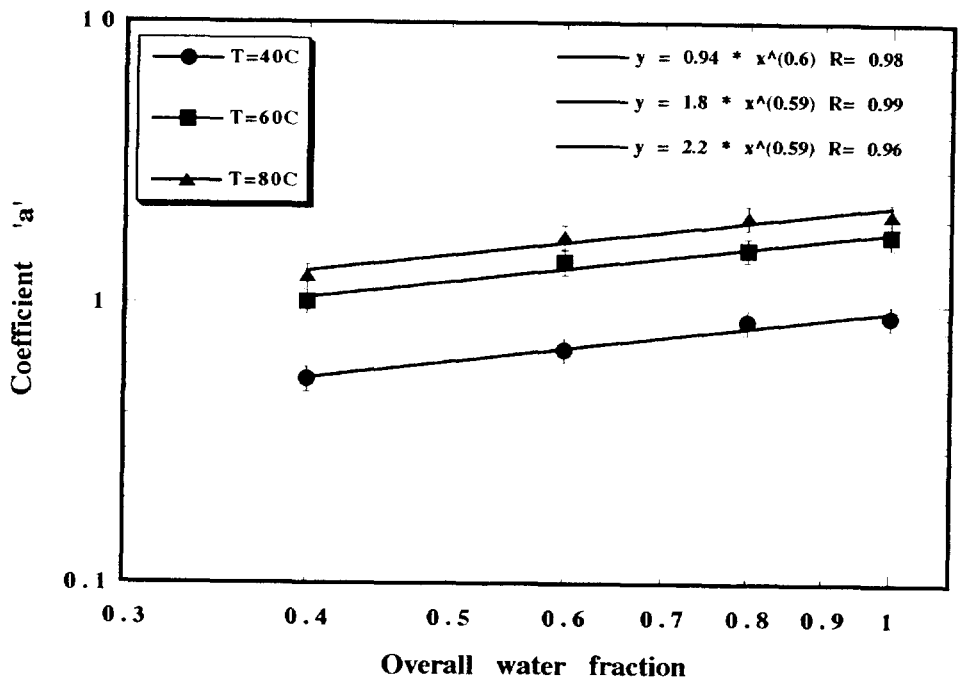

Figure 13. Coefficient 'a' vs overall water fraction for carbon dioxide partial pressure of 0.27MPa

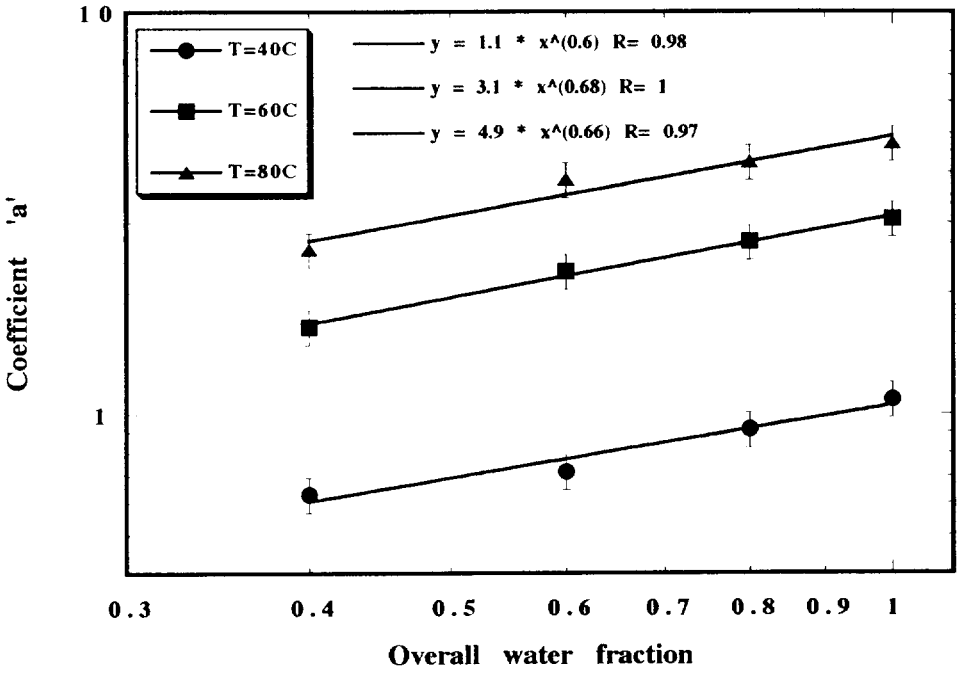

Figure 14. Coefficient 'a' vs overall water fraction for carbon dioxide partial pressure of 0.79MPa

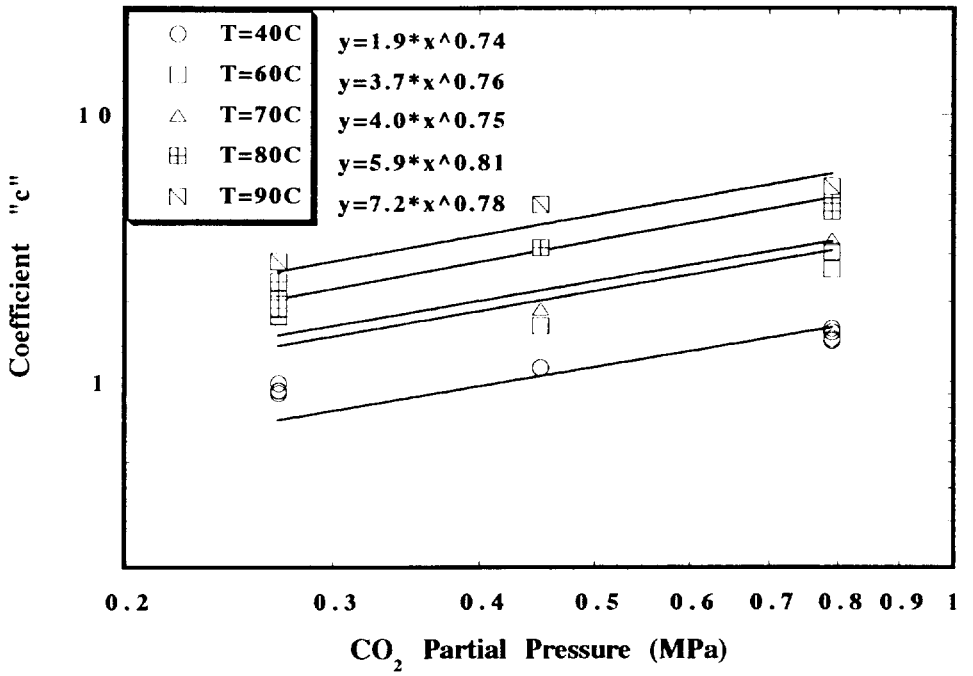

Figure 15. Coefficient "c" vs carbon dioxide partial pressure

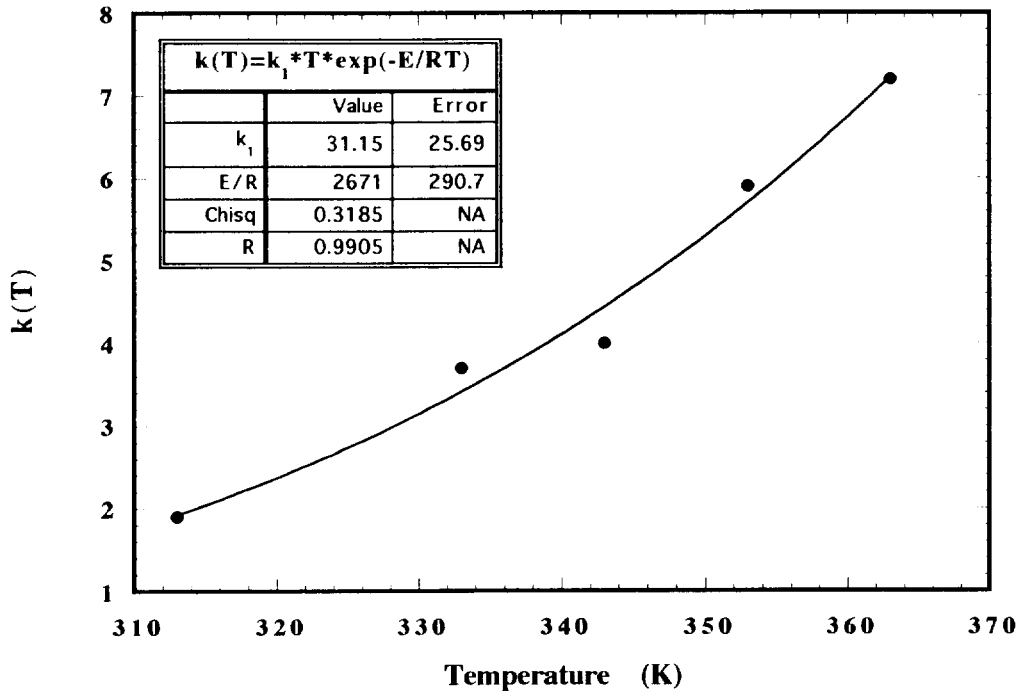

Figure 16. Coefficient 'k(T)' vs temperature

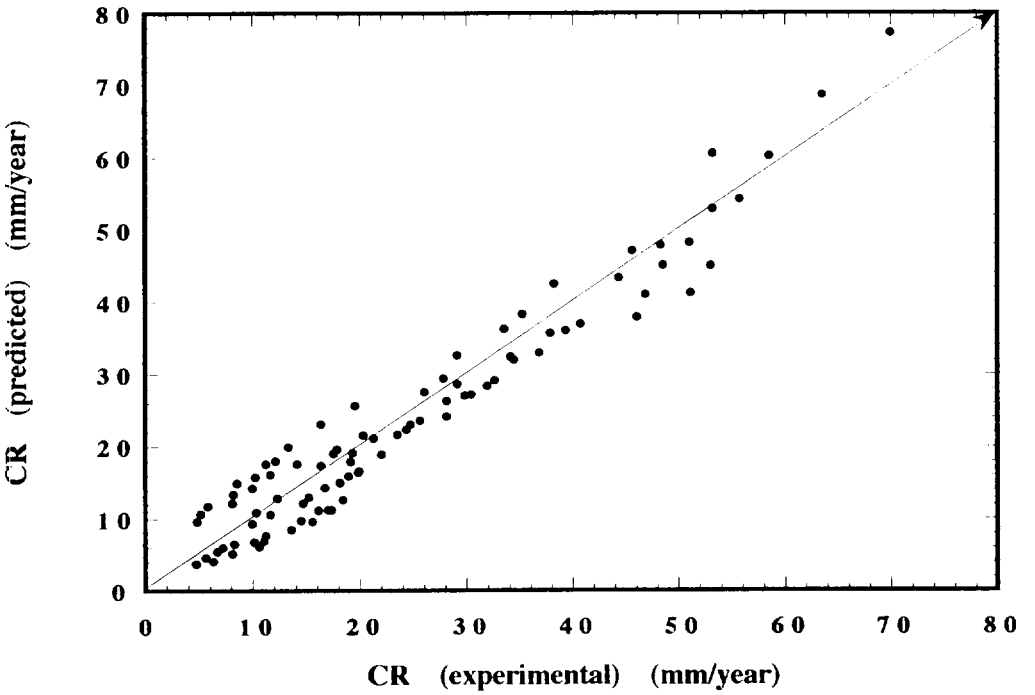

Figure 17. Predicted corrosion rates vs experimental corrosion rates for various oil compositions

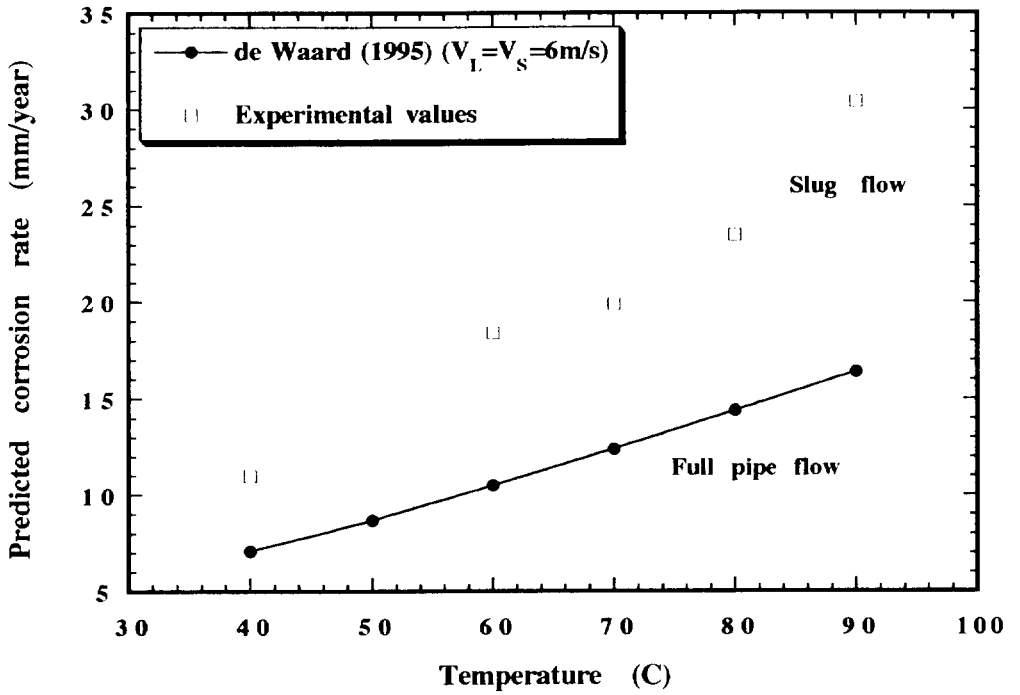

Figure 18. Predicted corrosion rate vs temperature for brine 0.27 MPa

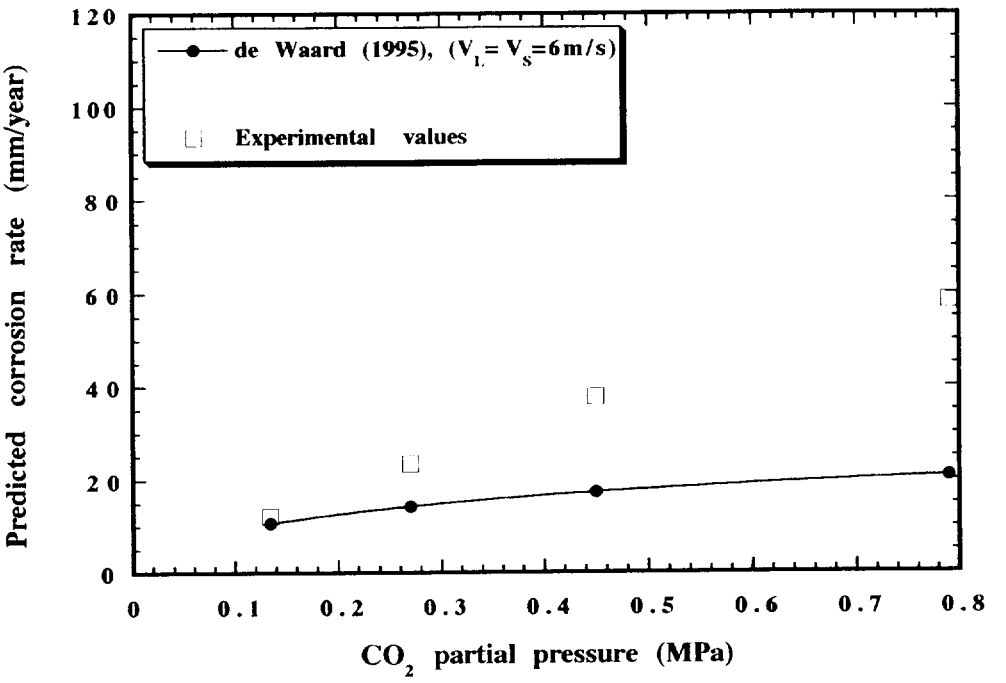

Figure 19. Predicted corrosion rates vs carbon dioxide partial pressure for brine at 80C.